Article

Bidentates versus Monodentates in Asymmetric Hydrogenation Catalysis: Synergic Effects on Rate and Allosteric Effects on Enantioselectivity

David W. Norman, Charles A. Carraz, David J. Hyett, Paul G. Pringle, Joseph B. Sweeney, A. Guy Orpen, Hirrahataya Phetmung, and Richard L. Wingad

J. Am. Chem. Soc., **2008**, 130 (21), 6840-6847 • DOI: 10.1021/ja800858x • Publication Date (Web): 03 May 2008

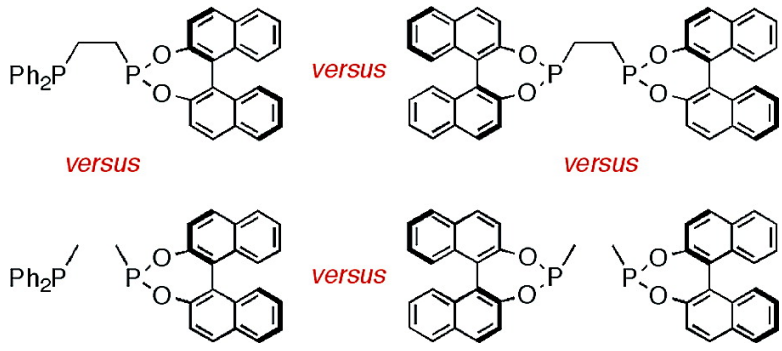

More About This Article

Additional resources and features associated with this article are available within the HTML version:

- Supporting Information
- Access to high resolution figures
- Links to articles and content related to this article
- Copyright permission to reproduce figures and/or text from this article

View the Full Text HTML

J|A|C|S
ARTICLES

Published on Web 05/03/2008

Bidentates versus Monodentates in Asymmetric Hydrogenation Catalysis: Synergic Effects on Rate and Allosteric Effects on Enantioselectivity

David W. Norman,[†] Charles A. Carraz,[†] David J. Hyett,[†,§] Paul G. Pringle,*[,†] Joseph B. Sweeney,[‡] A. Guy Orpen,[†] Hirrahataya Phetmung,[†] and Richard L. Wingad[†]

School of Chemistry, University of Bristol, Cantocks Close, Bristol BS8 1TS, U.K., and Department of Chemistry, University of Reading, Reading RG6 6AD, U.K.

Received February 3, 2008; E-mail: paul.pringle@bris.ac.uk

Abstract: C_1-Symmetric phosphino/phosphonite ligands are prepared by the reactions of $Ph_2P(CH_2)_2P(NMe_2)_2$ with (*S*)-1,1′-bi-2-naphthol (to give $\mathbf{L_A}$) or (*S*)-10,10′-bi-9-phenanthrol (to give $\mathbf{L_B}$). Racemic 10,10′-bi-9-phenanthrol is synthesized in three steps from phenanthrene in 44% overall yield. The complexes $[PdCl_2(\mathbf{L_{A,B}})]$ (**1a**,**b**), $[PtCl_2(\mathbf{L_{A,B}})]$ (**2a**,**b**), $[Rh(cod)(\mathbf{L_{A,B}})]BF_4$ (**3a**,**b**) and $[Rh(\mathbf{L_{A,B}})_2]BF_4$ (**4a**,**b**) are reported and the crystal structure of **1a** has been determined. A ^{31}P NMR study shows that **M**, a 1:1 mixture of the monodentates, $PMePh_2$ and methyl monophosphonite $\mathbf{L_{1a}}$ (based on (*S*)-1,1′-bi-2-naphthol), reacts with 1 equiv of $[Rh(cod)_2]BF_4$ to give the heteroligand complex $[Rh(cod)(PMePh_2)(\mathbf{L_{1a}})]BF_4$ (**5**) and homoligand complexes $[Rh(cod)(PMePh_2)_2]BF_4$ (**6**) and $[Rh(cod)(\mathbf{L_{1a}})_2]BF_4$ (**7**) in the ratio 2:1:1. The same mixture of **5**−**7** is obtained upon mixing the isolated homoligand complexes **6** and **7** although the equilibrium is only established rapidly in the presence of an excess of $PMePh_2$. The predominant species **5** is a monodentate ligand complex analogue of the chelate **3a**. When the mixture of **5**–**7** is exposed to 5 atm H_2 for 1 h (the conditions used for catalyst preactivation in the asymmetric hydrogenation studies), the products are identified as the solvento species $[Rh(PMePh_2)(\mathbf{L_{1a}})(S)_2]BF_4$ (**5′**), $[Rh(S)_2(PMePh_2)_2]BF_4$ (**6′**) and $[Rh(S)_2(\mathbf{L_{1a}})_2]BF_4$ (**7′**) and are formed in the same 2:1:1 ratio. The reaction of **M** with 0.5 equiv of $[Rh(cod)_2]BF_4$ gives exclusively the heteroligand complex *cis*-$[Rh(PMePh_2)_2(\mathbf{L_{1a}})_2]BF_4$ (**8**), an analogue of **4a**. The asymmetric hydrogenation of dehydroamino acid derivatives catalyzed by **3a**,**b** is reported, and the enantioselectivities are compared with those obtained with (a) chelate catalysts derived from analogous diphosphonite ligands $\mathbf{L_{2a}}$ and $\mathbf{L_{2b}}$, (b) catalysts based on methyl monophosphonites $\mathbf{L_{1a}}$ and $\mathbf{L_{1b}}$, and (c) catalysts derived from mixture **M**. For the cinnamate and acrylate substrates studied, the catalysts derived from the phosphino/phosphonite bidentates $\mathbf{L_{A,B}}$ generally give superior enantioselectivities to the analogous diphosphonites $\mathbf{L_{2a}}$ and $\mathbf{L_{2b}}$; these results are rationalized in terms of δ/λ-chelate conformations and allosteric effects of the substrates. The rate of hydrogenation of acrylate substrate **A** with heterochelate **3a** is significantly faster than with the homochelate analogues $[Rh(\mathbf{L_{2a}})(cod)]BF_4$ and $[Rh(dppe)(cod)]BF_4$. A synergic effect on the rate is also observed with the monodentate analogues: the rate of hydrogenation with the mixture containing predominantly heteroligand complex **5** is faster than with the monophosphine complex **6** or monophosphonite complex **7**. Thus the hydrogenation catalysis carried out with **M** and $[Rh(cod)_2]BF_4$ is controlled by the dominant and most efficient heteroligand complex **5**. In this study, the heterodiphos chelate **3a** is shown to be more efficient and gives the opposite sense of optical induction to the heteromonophos analogue **5**.

Introduction

In 2000, it was shown[1,2] that optically active monophosphonites based on 1,1′-bi-2-naphthol (binol), such as $\mathbf{L_{1a}}$, gave superior enantioselectivities to their bidentate analogues $\mathbf{L_{2a}}$ (Chart 1) in the rhodium-catalyzed asymmetric hydrogenations shown in eq 1. Moreover, we suggested[1] an explanation for

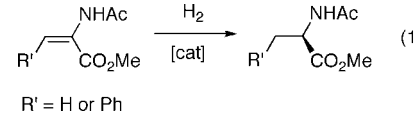

this phenomenon in terms of (i) restricted M−P rotations; (ii) the different orientation of the P−C bond in the monodentate and bidentate phosphonites; (iii) the *cis* preference of phosphonite ligands. These results overturned 25 years of dogma that bidentate phosphorus ligands consistently outperform their monodentate analogues.[3]

[†] University of Bristol.
[‡] University of Reading.
[§] Current address: DSM Research, P.O. Box 18, 6160 MD Geleen, The Netherlands.

(1) Claver, C.; Fernandez, E.; Gillon, A.; Heslop, K.; Hyett, D. J.; Martorell, A.; Orpen, A. G.; Pringle, P. G. *Chem. Commun.* **2000**, 961.
(2) Reetz, M. T.; Sell, T. *Tetrahedron Lett.* **2000**, *41*, 6333.

10.1021/ja800858x CCC: $40.75

Chart 1. *S*-Binol Derivatives only Shown

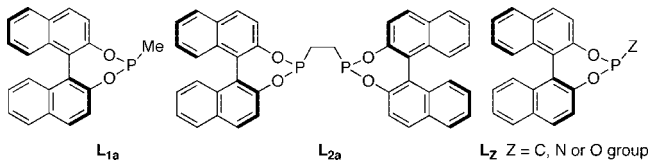

In the same year, Reetz et al.[4] reported that monophosphites ($\mathbf{L_Z}$, Z = OR) and de Vries, Feringa et al.[5] that monophosphoramidites ($\mathbf{L_Z}$, Z = NR_2) gave highly enantioselective hydrogenation catalysts (Chart 1). Both of these groups[6] and others[7] have subsequently shown that the design of chiral monophos ligands $\mathbf{L_Z}$ is amenable to high throughput screening techniques. (The term "monophos" is used throughout to mean a monodentate P-donor rather than the DSM trademarked "MonoPhos" family of phosphoramidite ligands.) One striking discovery has been that catalysts based on mixtures of monophos ligands $\mathbf{L_Z}$ and achiral PY_3 (Y = alkyl, aryl, or OR) can be more active and enantioselective than catalysts derived from monophos ligands $\mathbf{L_Z}$ alone.[8] This implies that, in some cases, the catalyst containing a Rh($\mathbf{L_Z}$)(PY_3) moiety is more active and selective than one containing a Rh($\mathbf{L_Z}$)$_2$ moiety. This approach has led to the development by the DSM group of a commercialized asymmetric hydrogenation process.[9]

The results of the catalysis with the mixed monodentate ligand systems are complicated to interpret because they depend on the proportions of the homoligand {Rh($\mathbf{L_Z}$)$_2$ and Rh(PY_3)$_2$} and heteroligand {Rh($\mathbf{L_Z}$)(PY_3)} catalysts present (and, in principle, the proportions of rhodium complexes with 0–4 P-donors coordinated[10]), the rates at which each of these catalyze the hydrogenation, and their enantioselectivity.[11,12] Not surprisingly therefore, the enantioselectivity is a sensitive function of $\mathbf{L_Z}$, the added PY_3, and the prochiral substrate. One advantage that bidentates have over monodentates is control over complex stoichiometry and stereochemistry: in general, a single, *cis*-chelate complex of stoichiometry M(diphos) is expected upon the addition of a diphos ligand to a metal catalyst precursor. Indeed several bidentate phosphine/phosphites[13,14] and phosphine/phosphoramidites[14,15] and a few phosphine/phosphonites[16] have been shown to form excellent chelate catalysts. However, a comparison of the performance of directly analogous heteromonophos and heterodiphos systems has not been reported.

Chart 2

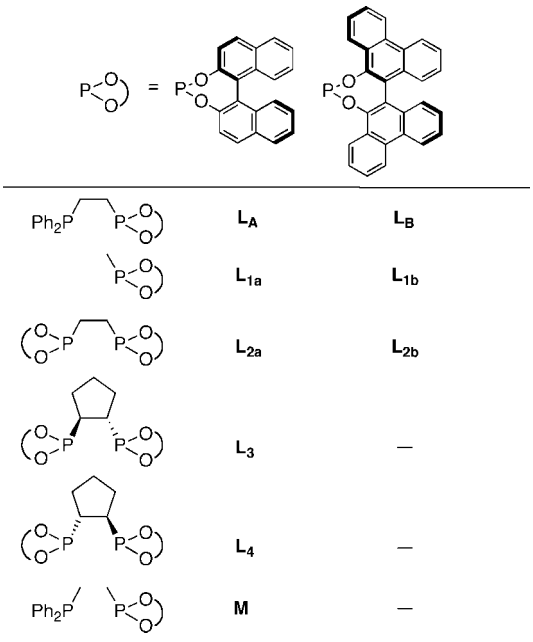

In this contribution, the factors that determine the asymmetric hydrogenation catalytic performance of rhodium complexes of mixed phosphine/phosphonite bidentate and monodentate ligands are probed by comparing the results obtained with catalysts derived from the ligands shown in Chart 2. The efficacy of the catalysts derived from the new, bidentate, phosphine/phosphonite ligands $\mathbf{L_A}$ and $\mathbf{L_B}$ is compared with the corresponding results for the catalysts derived from (i) the bis(phosphonites) $\mathbf{L_{2a}}$, $\mathbf{L_{2b}}$, $\mathbf{L_3}$, and $\mathbf{L_4}$,[1,17] (ii) the monophosphonites $\mathbf{L_{1a}}$ and $\mathbf{L_{1b}}$, and (iii) the mixture (**M**) of monophosphine $PMePh_2$ and monophosphonite $\mathbf{L_{1a}}$.

Results and Discussion

Ligand Synthesis. The phosphine/phosphonite ligands $\mathbf{L_A}$ and $\mathbf{L_B}$ were readily prepared by the route shown in eq 2 which is an adaptation of King's method[18] for making $Ph_2PCH_2CH_2P(OMe)_2$.

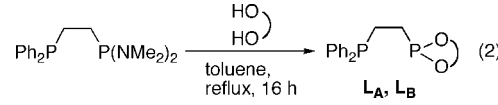

The amidophosphine precursor and optically active binol are commercially available. Racemic 10,10′-bi-9-phenanthrol (biphol) was synthesized as shown in Scheme 1 and resolved by Toda's method[19,20] (see Experimental Section).

(3) (a) Lagasse, F.; Kagan, H. B. *Chem. Pharm. Bull.* **2000**, *48*, 315. (b) Chaloner, P. A.; Esteruelas, M. A.; Joó, F.; Oro, L. A. *Homogeneous Hydrogenation*; Kluwer: London, 1994. (c) *The Handbook of Homogeneous Hydrogenation*; de Vries, J. G., Elsevier, C. J.,Eds.; Wiley-VCH: Weinheim, 2007.
(4) Reetz, M. T.; Mehler, G. *Angew. Chem., Int. Ed.* **2000**, *39*, 3889.
(5) van den Berg, M.; Minnaard, A. J.; Schudd, E. P.; van Esch, J.; de Vries, A. H. M.; de Vries, J. G.; Feringa, B. *J. Am. Chem. Soc.* **2000**, *122*, 11539.
(6) (a) de Vries, J. G.; Lefort, L. *Chem. Eur. J.* **2006**, *12*, 4722. and refs therein. (b) Reetz, M. T.; Mehler, G.; Meiswinkel, A. *Tetrahedron Asymmetry* **2004**, *15*, 2165. and refs therein.
(7) Jäkel, C.; Paciello, R. *Chem. Rev.* **2006**, *106*, 2912.
(8) (a) Hoen, R.; Boogers, J. A. F.; Bernsmann, H.; Ninnaard, A. J.; Meetsma, A.; Tiermersma-Wegman, T. D.; de Vries, A. H. M.; de Vries, J. G.; Feringa, B. L. *Angew. Chem., Int. Ed.* **2005**, *44*, 4208. (b) Reetz, M. T.; Bondarev, O. *Angew. Chem., Int. Ed.* **2007**, *46*, 4523.
(9) de Vries, A. H. M.; Lefort, L.; Boogers, J. A. F.; de Vries, J. G.; Ager, D. J. *Chim. Oggi* **2005**, *23*, 18.
(10) An IrP_1 complex has been shown to be the significant species in Ir-monophos-catalyzed asymmetric hydrogenations. Giacomina, F.; Meetsma, A.; Panella, L.; Lefort, L.; de Vries, A. H. M.; de Vries, J. G. *Angew. Chem., Int. Ed.* **2007**, *46*, 1497.
(11) Reetz, M. T.; Mehler, G. *Tetrahedron Lett.* **2003**, *44*, 4593.
(12) Reetz, M. T.; Fu, Y.; Meiswinkel, A. *Angew. Chem., Int. Ed.* **2006**, *45*, 1412.
(13) Nozaki, K. *Chem. Record* **2005**, *5*, 376. and refs therein.
(14) Zhang, W.; Chi, Y.; Zhang, X. *Acc. Chem. Res.* **2007**, *40*, 1278 and refs therein
(15) Wassenaar, J.; Reek, J. N. H. *Dalton Trans.* **2007**, 3750 and refs therein.
(16) (a) Schull, T. L.; Knight, D. A. *Tetrahedron Asymmetry* **1999**, *10*, 207. (b) Reetz, M. T.; Gosberg, A. *Tetrahedron Asymmetry* **1999**, *10*, 2129. (c) Laly, M.; Broussier, R.; Gautheron, B. *Tetrahedron Lett.* **2000**, *41*, 1183.
(17) (a) Dahlenburg, L. *Coord. Chem. Rev.* **2005**, *249*, 2962. and refs therein. (b) Dahlenburg, L. *Eur. J. Inorg. Chem.* **2003**, 2733. and refs therein.
(18) King, R. B.; Masler, W. F. *J. Am. Chem. Soc.* **1977**, *99*, 4001.
(19) Toda, F.; Tanaka, K. *J. Org. Chem.* **1988**, *53*, 3607.

Scheme 1

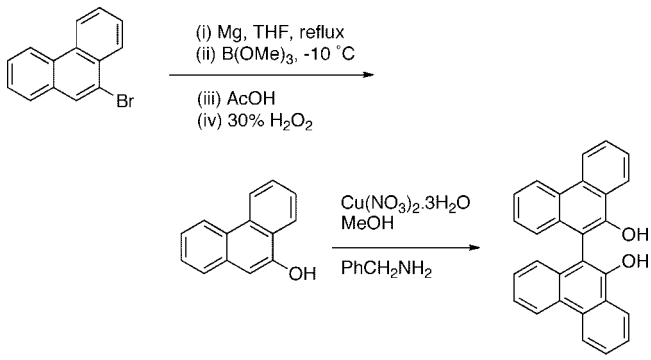

Scheme 2

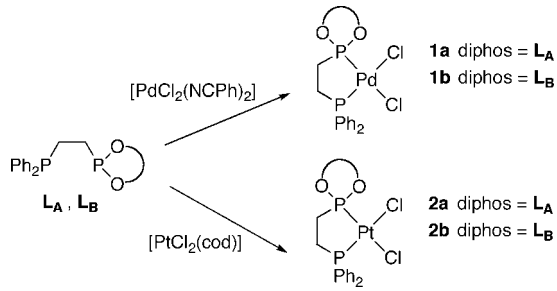

Ligands $\mathbf{L_A}$ and $\mathbf{L_B}$ are moderately air-sensitive solids but are indefinitely stable in an inert atmosphere. The ^{31}P NMR spectra of $\mathbf{L_A}$ and $\mathbf{L_B}$ were particularly informative of purity: in each case, two doublets were observed with ^3J(PP) $\approx$ 30 Hz. The individual δ(P) values for $\mathbf{L_A}$ ($-$11.8, $+$211.1) are similar to the symmetrical analogues, dppe ($-$12.5) and $\mathbf{L_{2a}}$ ($+$211.5).[1]

Coordination Chemistry. The palladium(II) and platinum(II) complexes **1a**,**b** and **2a**,**b** were made according to the routes shown in Scheme 2 (see Experimental Section for the characterizing data). Crystals of **1a** suitable for X-ray diffraction were grown by layering pentane on an acetonitrile solution of the complex and the crystal structure of **1a** as its acetonitrile solvate has been determined (Figure 1). The crystal system was triclinic, with two molecules of acetonitrile in the unit cell. In the crystal structure of **1a**, the five-membered chelate ring has a λ conformation. The Pd$-$P(binol) bond is significantly shorter than the Pd$-$PPh$_2$ bond.[21] The phosphonite donor apparently has a slightly higher *trans* influence than the phosphine donor in **1a**, since the Pd$-$Cl bond *trans* to the P(binol) donor is longer than the Pd$-$Cl *trans* to the PPh$_2$ donor albeit by less than 0.02 Å.[22]

The rhodium coordination chemistry of the heterodiphos ligands, $\mathbf{L_A}$ and $\mathbf{L_B}$, and the mixture of monophos ligands **M** was investigated because of its relevance to the asymmetric catalysis described below and is summarized in Schemes 3–5. The rhodium complexes **3a**,**b** were made by the reaction of 1 equiv of the corresponding $\mathbf{L_A}$ or $\mathbf{L_B}$ with [Rh(cod)$_2$]BF$_4$ (Scheme 3). The ^{31}P NMR data for the phosphine (δ 59.0, J(RhP) 154 Hz) and phosphonite (δ 206.8, J(RhP) 222 Hz) moieties in **3a** are similar to the data for the homochelates

Scheme 3

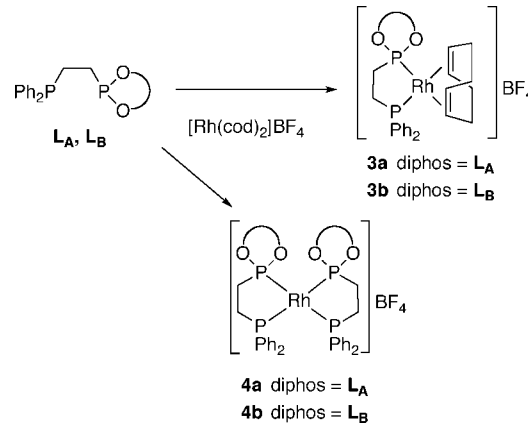

Scheme 4

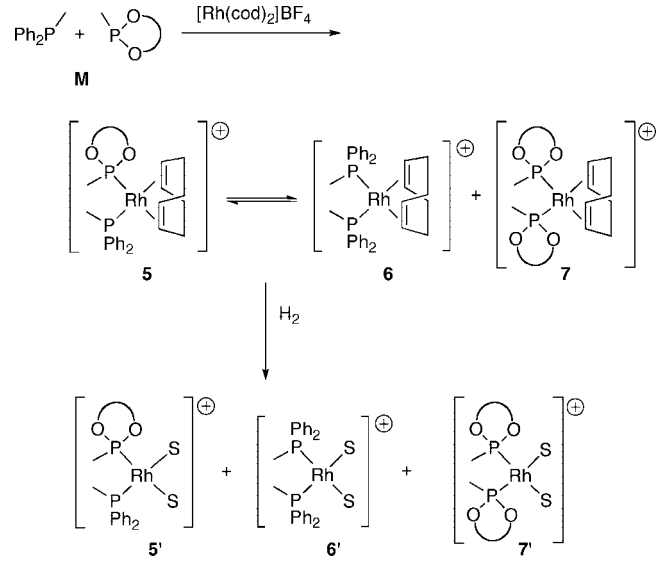

[Rh(cod)(dppe)]BF$_4$ (δ 56.5, J(RhP) 148 Hz)[23] and [Rh(cod)($\mathbf{L_{2a}}$)]BF$_4$ (δ 205.7, J(RhP) 229 Hz)[1] indicating that the P-environments in the heterochelate **3a** are similar to their homochelate analogues.

When more than 1 equiv of $\mathbf{L_A}$ or $\mathbf{L_B}$ was added to [Rh(cod)$_2$]BF$_4$, in each case a new product formed whose ^{31}P NMR spectrum was a symmetrical AA′MM′X pattern. The data (see Experimental Section) are consistent with the formation of the bis-chelates **4a** or **4b** in which the phosphine donors are mutually *cis*.

The products formed upon treatment of **M** with 1 equiv of [Rh(cod)$_2$]BF$_4$ were investigated by ^{31}P NMR spectroscopy. The spectrum obtained was consistent with the presence of complexes **5**$-$**7** (Scheme 4) in approximately the statistical 2:1:1 ratio. Precisely the same mixture of products was obtained after mixing the homoligand rhodium(I) complexes **6**[24] and **7**[1] in a 1:1 ratio in CH_2Cl_2. These experiments show that complexes **5**$-$**7** are in dynamic equilibrium (Scheme 4). The ^{31}P NMR data for the heteroligand complex **5** are similar to those for **3a** except the values of δ(P) are, as expected,[25] to low frequency of those for the five-membered chelate **3a**.

(20) An alternative procedure for the synthesis of optically active biphol has recently been reported. Ayudin, J.; Kumar, K. S.; Sayah, M. J.; Wallner, O. A.; Szabó, K. J. *J. Org. Chem.* **2007**, *72*, 4689.
(21) Atherton, M. J.; Fawcett, J.; Hill, A. P.; Holloway, J. H.; Hope, E. G.; Russell, D. R.; Saunders, G. C.; Stead, R. M. J. *J. Chem. Soc., Dalton Trans.* **1997**, 1137.
(22) Martín, A.; Orpen, A. G. *J. Am. Chem. Soc.* **1996**, *118*, 1464.
(23) de Wolf, E.; Spek, A. L.; Kuipers, B. W. M.; Philipse, A. P.; Meeldijk, J. D.; Bomans, P. H. H.; Frederik, P. M.; Deelman, B-J.; van Koten, G. *Tetrahedron* **2002**, *58*, 3911.
(24) Osborn, J. A.; Schrock, R. R. *J. Am. Chem. Soc.* **1971**, *93*, 2397.
(25) Appleton, T. G.; Bennett, M. A.; Tomkins, I. B. *J. Chem. Soc., Dalton Trans.* **1976**, 439.

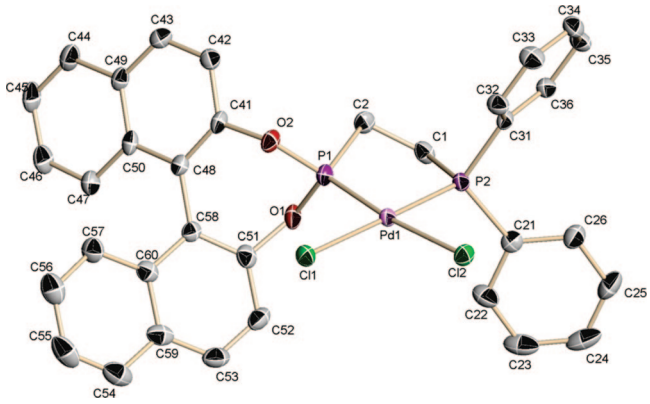

Figure 1. Solid-state molecular structure of **1a** (*S*-isomer). Hydrogen atoms have been omitted for clarity. Selected bond lengths (Å) and angles (deg): Pd(1)−P(1) = 2.1933(9), Pd(1)−P(2) = 2.2525(9), Pd(1)−Cl(1) = 2.3621(9), Pd(1)−Cl(2) = 2.3790(9), P(1)−O(1) = 1.607(2), P(1)−O(2) = 1.601(2), P(1)−C(2) = 1.807(4), P(2)−C(1) = 1.845(3), P(2)−C(21) = 1.818(4),P(2)−C(31)=1.822(3);P(1)−Pd(1)−P(2)=85.40(3),P(1)−Pd(1)−Cl(1) = 90.50(3), P(2)−Pd(1)−Cl(2) = 88.62(3), Cl(1)−Pd(1)−Cl(2) = 95.61(3).

It was noted that the equilibrium in Scheme 4 took up to 1 h to be established but was reduced to 5 min by the addition of $PMePh_2$ which catalyzes the ligand exchange. Thus, in order to obtain reproducible results in the hydrogenations with **M** (see below), the isolated complexes **6** and **7** were mixed in the presence of 0.1 equiv of $PMePh_2$. In addition, the catalyst was activated by submitting it to 5 atm of H_2 for 1 h to obviate any potential problems in interpreting the results due to 1,5-cyclooctadiene hydrogenation.[26] The ^{31}P NMR spectrum of the products of hydrogenation of the mixture of **5**–**7** showed the presence of three species in the ratio of 2:1:1 (see Scheme 4). The major component was assigned the structure **5′** on the basis of the AMX ^{31}P NMR pattern and the absence of hydride signals in the ^{1}H NMR spectrum of the mixture. The two minor products (doublets in the ^{31}P NMR spectrum) were assigned to the solvento complexes **6′** and **7′** (see Experimental Section for the data). It was apparent that the ratio in the **5**–**7** mixture was similar to the ratio of the derivatives **5′**–**7′**.

When the mixture **M** was added to 0.5 equiv of $[Rh(cod)_2]BF_4$ in CH_2Cl_2, a single species was formed and assigned the structure **8** (Scheme 5) on the basis of the AA′MM′X pattern in the ^{31}P NMR spectrum which was similar to that observed for the bis-chelate analogue **4a**. The same species **8** is also the product of the addition of $\mathbf{L_{1a}}$ to **6** or $PMePh_2$ to **7** (Scheme 5). Compound **8** was only detected when the ratio of mixture **M** to Rh exceeded 1:1. In the catalysis experiments below, an excess of **M** was avoided since we found that **8** had very low activity and gave essentially racemic hydrogenation products.

Asymmetric Hydrogenation Catalysis. The chelates **3a**,**b** were screened for asymmetric hydrogenation of the substrates **A**−**F** (Chart 3), and the results are collected in Table 1.

In general, the biphol-derived catalyst **3b** was more selective for these substrates than the binol-derived catalyst **3a**. The variation in the enantioselectivity with the cinnamic acid derivatives **B**−**F** (entries 1 and 2, Table 1) shows the sensitivity of the catalysts to subtle changes in the substrate structure. When

Scheme 5

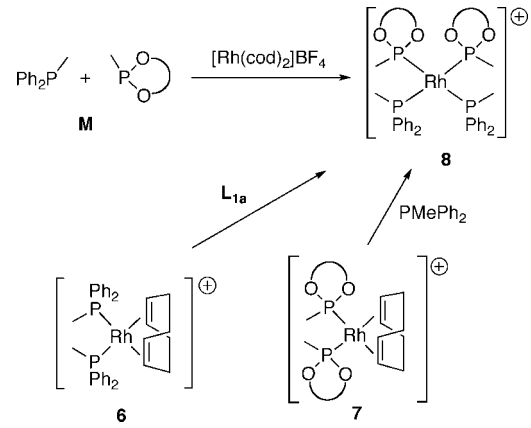

Table 1. Asymmetric Hydrogenations of Substrates **A**−**F**[a]

			substrate/ee[b]					
entry	ligand	catalyst	**A**	**B**	**C**	**D**	**E**	**F**
1	$\mathbf{L_A}$	**3a**	74	69	>99	78	72	n.d.
2	$\mathbf{L_B}$	**3b**	94	96	>99	n.d.	92	96
3	$\mathbf{L_A}$	in situ	53	57				
4	$\mathbf{L_A}$	**4a**	55	51				

[a] Conditions: in CH_2Cl_2, 5 bar H_2, 25 °C, 1 mol % catalyst, 1 h; conversions were 100% (see Experimental Section for full details). [b] The %*R* enantiomer formed in excess.

Chart 3

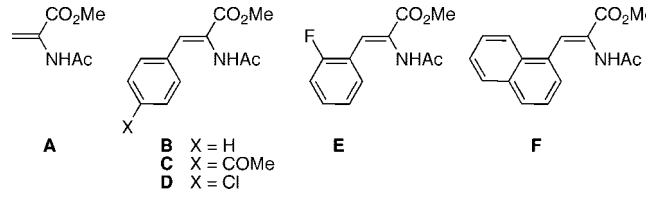

the catalyst used was made in situ by addition of $\mathbf{L_A}$ to $[Rh(cod)_2]BF_4$ rather than preformed **3a**, the rates of hydrogenation were slower and the ee was lower (entry 3, Table 1); in fact the results were similar to those obtained with the preformed bis-chelate **4a** (entry 4, Table 1). The hydrogenation of substrate **B** was carried out with preformed **3a** and **3b** at higher (25 atm) and lower (1 atm) pressure of H_2; this had no effect on the enantioselectivities, but the rates of hydrogenation were faster at higher H_2 pressure.

The efficiency of the heterochelate catalyst **3a** for hydrogenation of substrate **A** was compared with those of the homochelates $[Rh(cod)(\mathbf{L_{2a}})]BF_4$ and $[Rh(cod)(dppe)]BF_4$ by monitoring the substrate conversion as a function of time. Under the same reaction conditions (see Experimental Section), after 3 min, the conversion of substrate **A** using **3a** as catalyst was 95%, using $[Rh(cod)(\mathbf{L_{2a}})]BF_4$ as catalyst was 33%, and using $[Rh(cod)(dppe)]BF_4$ as catalyst was 8%. These experiments show that having a mixed P-donor set in this case leads to a significant enhancement in rate; we[27,28] and others[13] have previously noted a synergic effect on the rates of catalysis with mixed P-donor catalysts.

(26) Cobley, C. J.; Lennon, I. C.; McCague, R.; Ramsden, J. A.; Zanotti-Gerosa, A. *Tetrahedron Lett.* **2001**, *42*, 7481.

(27) Carraz, C. A.; Ditzel, E. J.; Orpen, A. G.; Ellis, D. D.; Pringle, P. G.; Sunley, G. J. *Chem. Commun.* **2000**, 1277.

(28) Basra, S.; de Vries, J. G.; Hyett, D. J.; Harrison, G.; Heslop, K. M.; Orpen, A. G.; Pringle, P. G.; von der Luehe, K. *Dalton Trans.* **2004**, 1901.

Table 2. Comparison of Asymmetric Hydrogenations of Substrates **A** and **B**[a]

entry	ligand[b]	ee[c] A	ee[c] B	ref
1	$\mathbf{L_A}$	74	69	this work
2	$\mathbf{L_B}$	94	96	this work
3	$\mathbf{L_{2a}}$	90	19	1
4	$\mathbf{L_{2b}}$	23	14	1
5	$\mathbf{L_3}$	89	85	17
6	$\mathbf{L_4}$	26	36	17
7	$\mathbf{L_{1a}}$	93	92	this work
8	$\mathbf{L_{1b}}$	29	−14	1
9	**M**[d]	−40	−27	this work

[a] Conditions in this work: 5 bar H_2, 25 °C, CH_2Cl_2 (unless otherwise stated), 1 mol % catalyst (see Experimental Section for full details). [b] Preformed rhodium complexes were used unless otherwise stated. [c] The *%R*-enantiomer formed in excess; a negative number indicates that the *S*-enantiomer was in excess. [d] This catalyst was generated by mixing complexes **6** and **7** (see Experimental Section) in a 5:1 mixture of EtOAc/CH_2Cl_2. In pure CH_2Cl_2, the ee was −14% with substrate **A** and −11% with substrate **B**.

The data collected in Table 2 will be used to discuss the results obtained for the asymmetric hydrogenations of substrates **A** and **B** with catalysts derived from the ligands shown in Chart 2.

The bidentate ligands $\mathbf{L_A}$, $\mathbf{L_B}$, $\mathbf{L_{2a}}$, and $\mathbf{L_{2b}}$ all contain the flexible PCH_2CH_2P unit which allows the metal chelate rings to adopt chiral δ and λ conformations (Figure 2a). Rapid ring inversion would be expected,[29] but these conformers will not be equally populated in solution because they are diastereoisomers, by virtue of the *S*-binol or *S*-biphol substitutents. In terms of the catalyst enantioselectivity, one of the diastereoisomers will be the matched isomer, and the other, the mismatched isomer. The ee obtained will depend on the relative abundance of the two diastereoisomers and their catalytic activity and enantioselectivity.

Dahlenburg[17] has convincingly demonstrated, with evidence from the *S*-binol-derived ligands $\mathbf{L_3}$ and $\mathbf{L_4}$ which have enforced δ and λ conformations (Figure 2b), that the δ chelate is the matched isomer, i.e. for the hydrogenation of substrates **A** and **B**, the catalyst derived from $\mathbf{L_3}$ gave higher *R*-enantioselectivity than the catalyst derived from $\mathbf{L_4}$ (see entries 5 and 6). They argued that upper-left/lower-right quadrant blocking (which favors *R*-enantioselectivity[30]) by the *S*-binol substituents was reinforced by the δ conformation of the chelate which puts the blocking groups in a more effective pseudoaxial site. The crystal structures of $[PdCl_2(\mathbf{L_A})]$ and $[PtCl_2(\mathbf{L_{2b}})]$[1] reproduced in Figure 3 corroborate this explanation: in the δ conformer $[PdCl_2(\mathbf{L_A})]$ (Figure 3a) the upper-left quadrant is clearly more blocked than in the λ conformer $[PtCl_2(\mathbf{L_{2b}})]$ (Figure 3b).

We suggest that solutions of the catalysts derived from $\mathbf{L_{2a}}$ and $\mathbf{L_{2b}}$ contain mixtures of matched (*S,S*-δ) and mismatched (*S,S*-λ) chelates (Figure 2a).[31] The high ee obtained in the hydrogenation of substrate **A** with the catalyst derived from $\mathbf{L_{2a}}$ is consistent with the catalyst behaving as the matched *S,S*-δ species (compare entries 3 and 5, Table 2) whereas the low ee obtained for substrate **B** with the same catalyst is consistent with the catalyst behaving as the mismatched *S,S*-λ species (entries 3 and 6, Table 2). It appears that the conformation (or shape) of the catalyst responds to the substrate, i.e., an allosteric effect.[32] Support for the suggestion that the substrate can influence the chelate conformation comes from the crystal structures of complexes of the type $[Rh(diphos)(\eta^4\text{-diene})]^+$ which show that the adoption of a δ or λ chelate conformation depends on the diene.[33]

There is a striking contrast between the high enantioselectivities obtained with biphol-heterochelate $[Rh(cod)(\mathbf{L_B})]BF_4$ (entry 2, Table 2) and the low enantioselectivities obtained with biphol-homochelate $[Rh(cod)(\mathbf{L_{2b}})]BF_4$ (entry 4, Table 2). As above, we suggest that at least part of the explanation for this is the difference in populations and/or activities of the matched and mismatched conformers.

Inspection of the enantioselectivities obtained with the catalysts derived from analogous monophosphonite and diphosphonite catalysts reveals complicated behavior. The catalyst derived from the binol-monodentate $\mathbf{L_{1a}}$ gave higher ee's (entry 7, Table 2) than the analogous diphos $\mathbf{L_{2a}}$ (entry 3, Table 2), whereas the biphol-derived monodentate $\mathbf{L_{1b}}$ and diphos $\mathbf{L_{2b}}$ both gave poor ee's (entries 4 and 8, Table 2). The greater conformational flexibility of monodentate P-complexes (via Rh−P rotation) than analogous diphos complexes coupled with an incomplete understanding of the mechanism of the hydrogenation with monodentate P-catalysts[10,34,35] makes interpretation of these enantioselectivities fraught with difficulties.

The distinction is clearer when the unsymmetrical diphos $\mathbf{L_A}$ (entry 1, Table 2) is compared with the mixture of monodentates **M** (entry 9, Table 2). The catalyst derived from the mixture **M** not only gives lower ee's than $\mathbf{L_A}$ but the sense of optical induction is opposite. Reetz et al. reported a similar inversion of optical induction with catalysts derived from mixtures of chiral phosphites and achiral phosphines.[11] Assuming the catalysts **5**–**7** act independently, the net *S*-selectivity must be due to the mixed monodentate complex **5** since **6** is achiral and **7** gives *R*-product (Entry 7, Table 2). To probe this further, the hydrogenation of **A** catalyzed by **6**, **7**, and the 2:1:1 mixture of **5**–**7** derived from **M** was monitored by measuring the conversions to product as a function of time. Under the same reaction conditions (see Experimental Section), with the same Rh concentrations, after 3 min, the conversions were, 95% using mixture **5**–**7** as catalyst, 50% using $[Rh(cod)(PMePh_2)_2]BF_4$ (**6**) as catalyst, and 60% using $[Rh(cod)(\mathbf{L_{1a}})_2]BF_4$ (**7**) as catalyst. Thus, as with the heterodiphos catalyst **3a**, the heteromonophos catalyst **5** shows a synergic effect of the mixed donors on the rate of catalysis. This kinetic advantage offers the prospect of phosphonite/phosphine mixtures being discovered that yield efficient and selective catalysts.

Conclusion

Monodentate P-ligands have made a great impact on asymmetric hydrogenation catalysis in recent years. From the discovery of

(29) Fernandez, E.; Gillon, A.; Heslop, K.; Horwood, E.; Hyettt, D. J.; Orpen, A. G.; Pringle, P. G. *Chem. Commun.* **2000**, 1663.
(30) Gridnev, I.; Imamoto, T. *Acc. Chem. Res.* **2004**, *37*, 633.
(31) The ^{31}P NMR spectrum of $[Rh(cod)(\mathbf{L_{2a}})]BF_4$ and $[Rh(cod)(\mathbf{L_A})]BF_4$ in CH_2Cl_2 solution showed only one set of signals even at −80°C; this could be because only one conformer is present at NMR-detectable levels or, more likely, that the λ and δ conformers are in rapid equilibrium with a low-energy barrier to ring inversion.
(32) (a) Allosteric effects are normally associated with enzyme catalysts although synthetic catalysts are known that show allosteric effects; see: Merlau, M. L.; Mejia, M. P.; Nguyen, S. T.; Hupp, J. T. *Angew. Chem., Int. Ed.* **2001**, *40*, 4239. (b) Gianneschi, N. C.; Bertin, P. A.; Nguyen, S. T.; Mirkin, C. A.; Zakharov, L. N.; Rheingold, A. L. *J. Am. Chem. Soc.* **2003**, *125*, 10508. (c) We have previously suggested an allosteric effect with an asymmetric hydrogenation catalyst; see: Baber, A.; de Vries, J. G.; Orpen, A. G.; Pringle, P. G.; von der Luehe, K. *Dalton Trans.* **2006**, 4821.
(33) Tsuruta, H.; Imamoto, T.; Yamaguchi, K.; Gridnev, I. D. *Tetrahedron Lett.* **2005**, *46*, 2879.
(34) Gridnev, I. D.; Fan, C.; Pringle, P. G. *Chem. Commun.* **2007**, 1319.

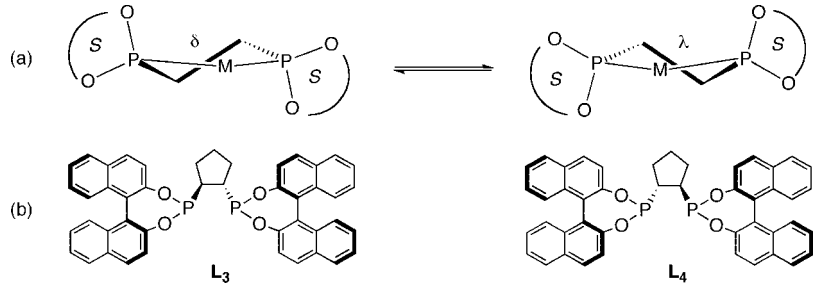

Figure 2. (a) Schematic of the δ/λ conformer equilibrium for a ligand with a flexible C_2-backbone; (b) Dahlensburg's ligands which give δ and λ chelate conformers respectively enforced by the rigid C_2-backbone.[17]

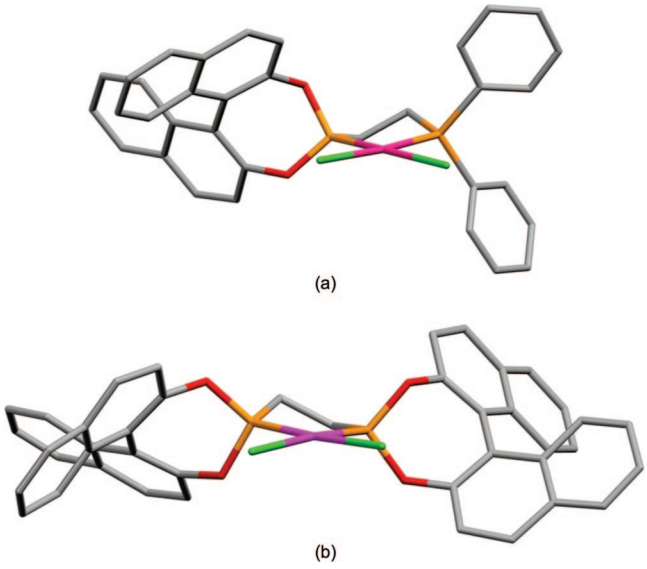

Figure 3. Crystal structures of (a) [$PdCl_2$($\mathbf{L_A}$)] (**1a**) and (b) [$PtCl_2$($\mathbf{L_{2b}}$)][1] (with phenanthrene fragments truncated for ease of comparison) showing the δ and λ chelate conformations and their effect on the upper-left quadrant blocking.

effective combinations of achiral and optically active monodentates has emerged a powerful high throughput protocol for tailoring catalysts to a particular substrate. The comparison of the heterobidentate phosphino/phosphonite $\mathbf{L_A}$ and the monophosphonite/monophosphine analogue **M** presented in this article has revealed that the greater activity of the heteroligand catalysts compared to that of the homoligand catalysts is true for the bidentate and monodentate systems. The synergic effect of the heteroligands on the rate explains why the heteromonodentates dominate the catalysis in mixed monodentate systems.

It is well-known that the performance of many asymmetric hydrogenation catalysts is sensitive to the substrate,[36] and here we have argued that chelate catalysts with flexible backbones will be particularly prone to this sensitivity because of substrate-induced conformational changes, i.e. allosteric effects. For example, the observation of the contrasting performances of the five-membered chelates formed by the diphosphonites $\mathbf{L_{2a}}$, $\mathbf{L_{2b}}$ and the phosphine/phosphonites $\mathbf{L_A}$, $\mathbf{L_B}$ can be partly explained by differences in populations and activities of matched (δ) and mismatched (λ) conformers of the chelate catalysts. Conformational preferences will certainly be important, but inevitably more difficult to predict, with the rotationally less constrained monodentate P-ligands, as implied by the opposite sense of induction observed with the heterodiphos and analogous heteromonophos systems described here. Further mechanistic studies aimed at deepening the understanding of these important features are in progress.[34]

Experimental Section

Unless otherwise stated, all work was carried out under a dry nitrogen atmosphere, using standard Schlenk line techniques. Dry N_2-saturated solvents were collected from a Grubbs system[37] in flame- and vacuum-dried glassware. Anhydrous methanol and pentane were purchased from Aldrich and were degassed prior to use by bubbling with dry nitrogen. 2,2-Dimethoxypropane was freshly distilled prior to use. [$PtCl_2$(cod)],[38] [$PdCl_2$($NCPh)_2$],[39] and [$Rh(cod)_2$]BF_4,[40] were prepared by literature methods. (*S*)-(−)-1,1′-bi-2-naphthol was purchased from Syncom BV, Groningen and $Ph_2P(CH_2)_2P(NMe_2)_2$ was purchased from EPP Ltd. (Edinburgh). Substrates **C**−**F** were supplied by DSM chemicals. All other starting materials were purchased from Aldrich. Unless otherwise stated, ^{1}H, ^{13}C, and ^{31}P NMR spectra were recorded at 300, 75, and 121 MHz respectively at +23 °C on a Jeol ECP 300 spectrometer. Mass spectra were recorded on a Fisons MD800 (FAB), a VG Analytical Quattro (ESI) or a VG Analytical Autospec (EI). Elemental analyses were carried out by the Microanalytical Laboratory of the School of Chemistry, University of Bristol.

9-Hydroxyphenanthrene. This precursor was prepared in pure form for the coupling reaction to racemic 10,10′-bi-9-phenanthrol described below since the commercially available technical grade of 9-hydroxyphenanthrene was found to be unsuitable for the coupling reaction. Magnesium turnings (2.08 g, 86 mmol) were activated overnight by vigorous stirring under nitrogen. A dropping funnel was charged with a solution of 9-bromophenanthrene (20.04 g, 78 mmol) in tetrahydrofuran (65 cm^3). Enough of this solution was added to cover the magnesium turnings followed by the rest of the solution dropwise. After the addition, the mixture was refluxed for 20 h followed by cooling to room temperature to give the Grignard reagent. In a separate flask a solution of trimethylborate (9.6 cm^3, 86 mmol) in tetrahydrofuran (65 cm^3) was cooled to −10 °C, and the Grignard was added dropwise while maintaining the temperature below 0 °C. The solution was stirred for 1 h at −5 °C and then recooled to −10 °C. Glacial acetic acid (7 cm^3) was added followed by a solution of 30% aqueous hydrogen peroxide (8.7 cm^3) in water (7.9 cm^3) while maintaining the solution at <0 °C. The resulting brown solution was allowed to warm to room temperature while stirring for an additional 40 min. Saturated aqueous ammonium chloride solution was added (100 cm^3) followed by tetrahydrofuran (50 cm^3), and the organic layer

(35) Reetz, M. T.; Meiswinkel, A.; Mehler, G.; Angermund, K.; Graf, M.; Thiel, T.; Mynott, R.; Blackmond, D. G. *J. Am. Chem. Soc.* **2005**, *127*, 10305.
(36) Tang, W.; Zhang, X. *Chem. Rev.* **2003**, *103*, 3029.
(37) Pangborn, A. B.; Giardello, M. A.; Grubbs, R. H.; Rosen, R. K.; Timmers, F. J. *Organometallics* **1996**, *15*, 1518.
(38) McDermott, J. X.; White, J. F.; Whitesides, G. M. *J. Am. Chem. Soc.* **1976**, *98*, 6521.
(39) Doyle, J. R.; Slade, P. E.; Jonassen, H. B. *Inorg. Synth.* **1960**, *6*, 218.
(40) Schenk, T. G.; Downes, J. M.; Milne, C. R. C.; MacKenzie, P. B.; Boucher, H.; Whelan, J.; Bosnich, B. *Inorg. Chem.* **1985**, *24*, 2334.

was separated. The organic layer was washed with saturated aqueous sodium bicarbonate solution (100 cm^3), water (100 cm^3), and brine (3 × 100 cm^3), dried with magnesium sulfate, and filtered. The solvent was removed in vacuo to yield a brown oil. This oil was dissolved in toluene, and the solvent was removed in vacuo to give 9-hydroxyphenanthrene as a light-brown powder (13.77 g, 71 mmol, 91%). The product can be recrystallized from toluene. Melting point: 134–136 °C; MS(EI): m/z = 194 (M^+); ^{1}H (270 MHz, $CDCl_3$) δ: 5.30 (s, 1H, O*H*), 7.02 (s, 1H, Ar*H*), 7.47–7.57 (m, 2H, Ar*H*), 7.62–7.73 (m, 3H, Ar*H*), 8.30–8.33 (m, 1H, Ar*H*), 8.58–8.70 (m, 2H, Ar*H*).

Racemic 10,10′-Bi-9-phenanthrol. Copper(II) nitrate trihydrate (5.00 g, 21 mmol) was added to a stirred solution of 9-hydroxyphenanthrene (2.01 g, 10 mmol) in methanol (50 cm^3) at room temperature. Benzylamine (6.8 cm^3, 62 mmol) was added to the deep-blue solution to give a thick brown suspension. The reaction mixture was stirred under nitrogen overnight and then quenched with a 2 M solution of hydrochloric acid (40 cm^3) to afford a thick blue-white suspension. The layers were partitioned by the addition of brine (50 cm^3) and CH_2Cl_2 (50 cm^3). The organic layer was separated and washed with 2 M aqueous ammonium hydroxide solution until the aqueous layer remained colorless. The organic layer was then washed with brine (2 × 100 cm^3), dried with magnesium sulfate, and filtered, and the solvent was removed in vacuo to give racemic 10,10′-bi-9-phenanthrol as a yellow solid (1.78 g, 4.6 mmol, 89%). Melting point: 231–233 °C; MS(EI): m/z = 386 (M^+), 368 ($M - 18^+$);^{1}H ($CDCl_3$) δ: 5.50 (2H, s, O*H*), 7.27 (2H, dd, ^3J(HH) = 8.4 Hz, ^4J(HH) = 1.2 Hz, Ar*H*), 7.35 (2H, ddd, ^3J(HH) = 8.2 Hz, $^3J'$(HH) = 6.9 Hz, ^4J(HH) = 1.2 Hz, Ar*H*), 7.54 (2H, ddd, ^3J(HH) = 8.3 Hz, $^3J'$(HH) = 6.8 Hz, ^4J(HH) = 1.5 Hz, Ar*H*), 7.72 (2H, ddd, ^3J(HH) = 8.2 Hz, $^3J'$(HH) = 7.0 Hz, ^4J(HH) = 1.2 Hz, Ar*H*), 7.82 (2H, ddd, ^3J(HH) = 8.3 Hz, $^3J'$(HH) = 7.0 Hz, ^4J(HH) = 1.4 Hz, Ar*H*), 8.46 (2H, dd, ^3J(HH) = 8.1 Hz, ^4J(HH) = 1.1 Hz, Ar*H*), 8.75 (2H, d, ^3J(HH) = 8.3 Hz, Ar*H*), 8.81 (2H, d, ^3J(HH) = 8.3 Hz, Ar*H*). The 10,10′-bi-9-phenanthrol was resolved using Toda's procedure.[19]

Preparation of L_A. $Ph_2P(CH_2)_2P(NMe_2)_2$ (1.15 g, 3.46 mmol) was dissolved in toluene (50 cm^3), and (*S*)-(−)-1,1′-bi-2-naphthol (0.99 g, 3.46 mmol) was added. The reaction mixture was refluxed for 16 h, and the solvent was removed in vacuo to give a white foamy solid. Trituration with pentane afforded $\mathbf{L_A}$ as a white solid (1.74 g, 3.29 mmol, 95%). MS(EI): m/z = 528 (M^+); HRMS(EI): calculated for $C_{34}H_{26}O_2P_2$: 528.1408, found 528.1401; ^{31}P{^{1}H} ($CDCl_3$) δ: −11.8 (d, ^3J(PP) = 28 Hz, *P*Ph_2), 211.1 (d, ^3J(PP) = 28 Hz, *P*(binol)); ^{1}H ($CDCl_3$) δ: 1.56–1.74 (2H, m, C*H*$_2$PPh$_2$), 2.10–2.27 (2H, m, C*H*$_2$P(binol)), 7.04–7.44 (18H, m, Ar*H*), 7.70–7.97 (4H, m, Ar*H*); ^{13}C{^{1}H} (100 MHz, $CDCl_3$) δ: 19.63 (dd, ^1J(PC) = 16.9 Hz, ^2J(PC) = 14.6 Hz, *C*H$_2$PPh$_2$), 29.94 (dd,^1J(PC) = 36.9 Hz, ^2J(PC) = 14.6 Hz, *C*H$_2$P(binol)), 121.39 (d, J(PC) = 1.5 Hz), 122.00 (s), 123.62 (d, J(PC) = 3.1 Hz), 124.71 (d, J(PC) = 5.4 Hz), 125.03 (d, J(PC) = 6.9 Hz), 126.39 (s), 126.98 (d, J(PC) = 3.8 Hz), 128.40 (s), 128.50 (s), 128.56 (s), 128.65 (d, J(PC) = 2.3 Hz), 128.72 (s), 128.84 (s), 129.02 (s), 129.16 (s), 129.94 (s), 130.79 (s), 131.15 (s), 131.61 (s), 132.65 (s), 132.83 (s), 132.92 (s), 132.97 (s), 133.15 (s), 137.93 (d, J(PC) = 1.5 Hz), 138.06 (d, J(PC) = 1.5 Hz), 148.41 (d, J(PC) = 6.9 Hz, *C*−O), 150.30 (d, J(PC) = 3.1 Hz, *C*−O′).

Preparation of L_B. Prepared similarly to $\mathbf{L_A}$ from (*S*)-(−)-10,10′-bi-9-phenanthrol to give $\mathbf{L_B}$ as a pale-yellow solid (0.578 g, 0.92 mmol, 97%). MS(EI): m/z = 628 (M^+); HRMS(EI): calculated for $C_{42}H_{30}O_2P_2$: 628.1721, found 628.1723; ^{31}P{^{1}H} ($CDCl_3$) δ: −11.9 (d, ^3J(PP) = 28 Hz, *P*Ph_2), 216.2 (d, ^3J(PP) = 28 Hz, *P*(biphol)); ^{1}H ($CDCl_3$) δ: 1.67–1.79 (2H, m, C*H*$_2$PPh$_2$), 2.06–2.18 (1H, m, C*H*H′P(biphol)), 2.30–2.40 (1H, m, CH*H*′P(biphol)), 7.14–7.39 (14H, m, Ar*H*), 7.35–7.62 (2H, m, Ar*H*), 7.66 (1H, td, ^3J(HH) = 7.6 Hz, ^4J(HH) = 1.0 Hz, Ar*H*), 7.73 (1H, td, ^3J(HH) = 7.6 Hz, ^4J(HH) = 1.0 Hz, Ar*H*), 7.75–7.81 (2H, m, Ar*H*), 8.19 (1H, dd, ^3J(HH) = 8.1 Hz, ^4J(HH) = 1.1 Hz, Ar*H*), 8.35 (1H, dd, ^3J(HH) = 7.8 Hz, ^4J(HH) = 1.4 Hz, Ar*H*), 8.76 (2H, dd, ^3J(HH) = 8.2 Hz, ^4J(HH) = 2.5 Hz, Ar*H*), 8.79 (2H, d, ^3J(HH) = 8.2 Hz, Ar*H*); ^{13}C{^{1}H} ($CDCl_3$) δ: 19.53 (dd, ^1J(CP) = not resolved, ^2J(CP) = 14.9 Hz, *C*H$_2$PPh$_2$), 31.72 (dd, ^1J(CP) = 37.4 Hz, ^2J(CP) = 13.3 Hz, *C*H$_2$P(biphol)), 121.25 (d, J(CP) = 3.4 Hz), 121.91 (d, J(PC) = 5.8 Hz), 123.06 (s), 123.10 (d, J(PC) = 1.7 Hz), 125.48 (s), 125.84 (s), 125.88 (s), 126.69 (s), 126.77 (s), 127.24 (d, J(PC) = 1.2 Hz), 127.36 (s), 127.41 (s), 127.87 (s), 127.93 (s), 128.01 (s), 128.10 (s), 128.40 (s), 128.51 (s), 128.56 (s), 128.60 (s), 128.65 (s), 128.78 (s), 128.85 (s), 129.21 (s), 131.46 (d, J(PC) = 1.2 Hz), 131.64 (d, J(PC) = 1.2 Hz), 131.72 (d, J(PC) = 1.7 Hz), 132.07 (s), 132.59 (s), 132.68 (s), 132.83 (s), 132.94 (s), 137.66 (d, J(PC) = 13.3 Hz), 137.97 (d, J(PC) = 13.3 Hz), 146.05 (d, J(PC) = 8.1 Hz, *C*−O), 147.06 (d, J(PC) = 3.5 Hz, *C*−O′).

[$PdCl_2(L_A)$] (1a). To a solution of [$PdCl_2$(NCPh)$_2$] (90 mg, 0.23 mmol) dissolved in CH_2Cl_2 (2 cm^3) was added a solution of $\mathbf{L_A}$ (124 mg, 0.23 mmol) in CH_2Cl_2 (2 cm^3). After stirring the mixture for 1 h the volatiles were removed in vacuo. The residue was redissolved in CH_2Cl_2 (2 cm^3) and filtered through Celite. The Celite was washed with CH_2Cl_2 (10 cm^3), and the volume of the resultant solution was concentrated to ∼2 cm^3. Diethyl ether (10 cm^3) was added to precipitate an orange solid. The solid was filtered, washed with diethyl ether (2 × 10 cm^3), and dried in vacuo to give **1a** as a pale-orange solid (96 mg, 0.14 mmol, 61%). Elemental analysis (calcd): C, 57.98 (57.86); H, 3.83 (3.71); MS(FAB): m/z = 706 (M^+), 671 ($M^+ - {}^{35}$Cl);^{31}P{^{1}H} ($CDCl_3$) δ: 65.5 (^2J(PP) = 12.1 Hz, *P*Ph_2), 182.3 (^2J(PP) = 12.1 Hz, *P*(binol)); ^{1}H (CD_2Cl_2) δ: 1.84–2.61 (4H, m, C*H*$_2$C*H*$_2$), 7.04–8.21 (22H, m, Ar*H*).

[$PdCl_2(L_B)$] (1b). The complex was prepared similarly to **1a** from $\mathbf{L_B}$ to give **1b** as a white powder (43 mg, 0.05 mmol, 70%). Elemental analysis (calcd **1b**·2CH_2Cl_2): C, 53.99 (54.16); H, 3.59 (3.51); MS(FAB): m/z = 805 (M^+), 770 (M^+ − Cl), 735 (M^+ − 2Cl);^{31}P{^{1}H} (D_6-dmso) δ: 69.2 (^2J(PP) = 14.9 Hz, *P*Ph_2), 192.8 (^2J(PP) = 14.9 Hz, *P*(biphol)); ^{1}H (D_6-dmso) δ: 2.35–3.15 (4H, m, C*H*$_2$C*H*$_2$), 7.10 (1H, d, J = 8.1 Hz, Ar*H*), 7.18 (1H, d, J = 8.4 Hz, Ar*H*), 7.30–7.37 (2H, m, Ar*H*), 7.53–7.77 (10H, m, Ar*H*), 7.80–7.92 (4H, m, Ar*H*), 7.95–8.04 (2H, m, Ar*H*), 8.07 (1H, d, J = 8.1 Hz, Ar*H*), 8.41 (1H, d, J = 8.2 Hz, Ar*H*), 8.91–8.97 (3H, m, Ar*H*), 9.01 (1H, d, J = 8.4 Hz, Ar*H*).

[$PtCl_2(L_A)$] (2a). To a solution of [$PtCl_2$(cod)] (88 mg, 0.23 mmol) dissolved in CH_2Cl_2 (4 cm^3) was added a solution of $\mathbf{L_A}$ (124 mg, 0.23 mmol) in CH_2Cl_2 (3 cm^3). After stirring the mixture for 1 h, the solution was concentrated to ∼2 cm^3, and diethyl ether (10 cm^3) was added to precipitate a white solid. The solid was filtered, washed with diethyl ether (2 × 10 cm^3), and dried in vacuo to give **2a** as a white solid (151 mg, 0.19 mmol, 83%). Elemental analysis (calcd **2a**·Et_2O): C, 52.73 (52.60); H, 3.99 (4.07); MS(FAB): m/z = 759 ($M^+ - {}^{35}$Cl); ^{31}P{^{1}H} (CD_2Cl_2) δ: 43.3 (^1J(PtP) = 3500 Hz,^2J(PP) = 1.9 Hz, *P*Ph_2), 153.3 (^1J(PtP) = 5031 Hz,^2J(PP) = 1.9 Hz, *P*(binol));^{1}H (CD_2Cl_2) δ: 1.83–2.59 (4H, m, C*H*$_2$C*H*$_2$), 7.15–8.06 (22H, m, Ar*H*).

[$PtCl_2(L_B)$] (2b). The complex was prepared similarly to **2b** from $\mathbf{L_B}$ to give **2b** as a white powder (107 mg, 0.12 mmol, 63%). Elemental analysis (calcd **2b**·CH_2Cl_2): C, 52.29 (52.72); H, 3.41 (3.29); MS(FAB): m/z = 894 (M^+), 859 (M^+ − Cl);^{31}P{^{1}H} (D_6-dmso) δ: 44.8 (^1J(PtP) = 3465 Hz, ^2J(PP) not observed, *P*Ph_2), 160.9 (^1J(PtP) = 5066 Hz, ^2J(PP) not observed, *P*(biphol)); ^{1}H (D_6-dmso) δ: 2.23–2.41 (2H, m, C*H*$_2$PPh$_2$), 2.67–3.09 (2H, m, C*H*$_2$P(biphol)), 7.19 (1H, d, J = 7.7 Hz, Ar*H*), 7.27 (1H, d, J = 8.1 Hz, Ar*H*), 7.39 (1H, d, J = 8.4 Hz, Ar*H*), 7.44 (1H, d, J = 7.7 Hz, Ar*H*), 7.59–8.10 (16H, m, Ar*H*), 8.18 (1H, d, J = 7.9 Hz, Ar*H*), 8.46 (1H, d, J = 8.1 Hz, Ar*H*), 8.97–9.04 (3H, m, Ar*H*), 9.06 (1H, d, J = 8.2 Hz, Ar*H*).

[Rh(cod)(L_A)]BF_4 (3a). To a solution of [Rh(cod)$_2$]BF_4 (321 mg, 0.79 mmol) dissolved in CH_2Cl_2 (2 cm^3) was added a solution of $\mathbf{L_A}$ (418 mg, 0.79 mmol) in CH_2Cl_2 (10 cm^3) dropwise over 5 min. The resulting yellow solution was stirred for a further 30 min, and then the solution was concentrated to ∼5 cm^3, and the orange solid product **3a** precipitated by the addition of Et_2O (∼15 cm^3). The product **3a** was filtered off and dried in vacuo (500 mg, 0.61 mmol, 77%). Elemental analysis (calcd): C, 61.30 (61.04); H, 5.05

(4.63); MS(FAB): m/z = 739 ($M^+ - BF_4$), 631 ($M^+ - BF_4$ − cod); $^{31}P\{^1H\}$ ($CDCl_3$) δ: 59.0 (dd,^1J(RhP) = 154 Hz, ^2J(PP) = 27 Hz, *P*Ph_2), 206.8 (dd,^1J(RhP) = 222 Hz, ^2J(PP) = 27 Hz, *P*(binol)); ^1H ($CDCl_3$) δ: 2.07–2.70 (12H, m, CH_2CH_2 and 4 CH_2 groups from cod), 4.43 (1H, br, cod-C*H*), 5.09 (1H, br, cod-C*H*), 5.42 (1H, br, cod-C*H*), 5.74 (1H, br, cod-C*H*), 7.13–8.19 (22H, m, Ar*H*). In the presence of an excess of $\mathbf{L_A}$ complex **3a** reacts to form a new species assigned the bis-chelate structure **4a**. $^{31}P\{^1H\}$ (CH_2Cl_2) analyzed as an AA′MM′X spin system: δ_A: 218.7 (^1J(RhP) = 191.8 Hz, *P*(binol)), δ_M: 53.6 (^1J(RhP) = 127.5 Hz, *P*Ph_2), J(AM) = 333.1, J(AM′) = −30.7 Hz, J(AA′) = 31.9, J(MM′) = 22.6 Hz.

[Rh(cod)($\mathbf{L_B}$)]BF_4 (3b). The complex was prepared similarly to **3a** from $\mathbf{L_B}$ to give **3b** as an orange powder (145 mg, 0.16 mmol, 90%). Elemental analysis (calcd for **3b**·CH_2Cl_2·Et_2O): C, 60.44 (60.85); H, 4.73 (5.01); MS(EI): m/z = 838 ($M^+ - BF_4$); $^{31}P\{^1H\}$ ($CDCl_3$) δ: 57.3 (dd,^1J(RhP) = 154 Hz, ^2J(PP) = 27 Hz, *P*Ph_2), 209.3 (dd,^1J(RhP) = 223 Hz, ^2J(PP) = 27 Hz, *P*(biphol)); ^1H ($CDCl_3$) δ: 1.46–1.79 (12H, m, CH_2CH_2 and 4 CH_2 groups from cod), 3.86 (1H, br, cod-C*H*), 5.28 (2H, br, 2 cod-C*H*), 5.93 (1H, br, cod-C*H*), 7.30–7.98 (19H, m, Ar*H*), 8.24 (1H, d, J = 8.5 Hz, Ar*H*), 8.53 (1H, d, J = 8.5 Hz, Ar*H*), 8.77–8.86 (4H, m, Ar*H*), 8.87 (1H, d, J = 7.8 Hz, Ar*H*). In the presence of an excess of $\mathbf{L_B}$ complex **3b** reacts to form a new species assigned the bis-chelate structure **4b**. $^{31}P\{^1H\}$ (CH_2Cl_2) the AA′MM′X pattern was not fully analyzed: δ: 53.8 (^1J(RhP) = 125 Hz, |J(AM) + J(AM′)| = 306 Hz,*P*Ph_2), 223.0 (^1J(RhP) = 190 Hz, *P*(biphol)).

[Rh(cod)($\mathbf{L_{1a}}$)(P$MePh_2$)]BF_4 (5). Ligand mixture **M** was prepared by combining a solution of P$MePh_2$ (11 mg, 0.055 mmol) in CH_2Cl_2 (0.3 cm^3) with a solution of $\mathbf{L_{1a}}$ (18 mg, 0.055 mmol) in CH_2Cl_2 (0.3 cm^3) and was added to a NMR tube charged with [Rh(cod)$_2$]BF_4 (22 mg, 0.055 mmol) to give a light-orange solution of the products. $^{31}P\{^1H\}$ (CH_2Cl_2), major species **5**, δ: 14.8 (dd,^1J(RhP) = 146 Hz, ^2J(PP) = 40 Hz, *P*$MePh_2$), 192.4 (dd,^1J(RhP) = 211 Hz, ^2J(PP) = 40 Hz, *P*Me(binol)); minor species [Rh(cod)(P$MePh_2$)$_2$]BF_4 (**6**), δ: 11.4 (d,^1J(RhP) = 144 Hz) and [Rh(cod)($\mathbf{L_{1a}}$)$_2$]BF_4 (**7**), δ: 190.5 (d,^1J(RhP) = 208 Hz). The relative ratio of complexes **5**, **6**, and **7** remained constant after 1 h at 2:1:1. The same mixture of **5**–**7** was also made by mixing a solution of **6** (15 mg, 0.022 mmol) in CH_2Cl_2 (0.3 cm^3) and **7** (21 mg, 0.022 mmol) in CH_2Cl_2 (0.3 cm^3); with this method, equilibration took 1 h unless a trace (5–10%) of P$MePh_2$ was added when equilibrium was achieved in less than the time required to obtain an NMR spectrum of the reaction mixture (∼5 min).

[Rh($\mathbf{L_{1a}}$)$_2$(P$MePh_2$)$_2$]BF_4 (8). Ligand mixture **M** was prepared by combining a solution of P$MePh_2$ (22 mg, 0.11 mmol) in CH_2Cl_2 (0.3 cm^3) with a solution of $\mathbf{L_{1a}}$ (36 mg, 0.11 mmol) in CH_2Cl_2 (0.3 cm^3) and was added to a NMR tube charged with [Rh(cod)$_2$]BF_4 (22 mg, 0.055 mmol) to give a light-orange solution of the products. $^{31}P\{^1H\}$ (CH_2Cl_2) showed that *cis*-**8** was the product; the AA′MM′X pattern was not fully analyzed: δ: 13.0 (^1J(RhP) = 123.8 Hz, *P*$MePh_2$), 203.8 (^1J(RhP) = 187.0 Hz, |J(AM) + J(AM′)| = 294 Hz, *P*Me(binol)).

Asymmetric Hydrogenation of Substrate A. The catalyst (preformed complexes **3a**, **3b**, **4a**, **5**–**7** (0.0035 mmol)) and substrate **A** (0.35 mmol) were mixed in glass vessels under nitrogen; up to 10 vessels were placed in a parallel screening apparatus. CH_2Cl_2 was added (5 cm^3), the apparatus purged three times with hydrogen, and the autoclave then sealed and pressurized with hydrogen (5 bar). After 1 h of stirring the reaction mixtures, the autoclave was depressurised, and the reaction solutions were filtered through a small plug of silica and submitted for GC analysis using a Varian Chiracel-L-Val column (25 m × 0.25 mm × 0.12 μm) with He (carrier) at 1.5 cm^3/min, 112 °C.

Comparison of Rates of Asymmetric Hydrogenation of Substrate A. A stirred solution of the preformed catalyst (**3a**, [Rh(cod)(dppe)]BF_4, [Rh(cod)($\mathbf{L_{2a}}$)]BF_4, **5**, **6** or a mixture of **5**–**7**) (0.0035 mmol) in CH_2Cl_2 (1.0 cm^3) was preactivated by putting it under 5 atm of H_2 for 10 min in a 50 cm^3 glass autoclave. The pressure was then reduced to 1 atm H_2, a solution of substrate **A** (50.0 mg, 0.35 mmol) in ethyl acetate (4.0 cm^3) was added and the mixture stirred. Samples were taken at 0.5, 1, 3, 10, and 20 min and the conversions measured by GC analysis. All runs were done in duplicate.

Asymmetric Hydrogenation of Substrates B−F. The catalyst (preformed complexes **3a**, **3b**, **4a**, **5**–**7** or ligands $\mathbf{L_A}$ or $\mathbf{L_B}$ with equimolar amounts of [Rh(cod)$_2$]BF_4 (0.010 mmol)) and the substrates **B**−**F** (1.0 mmol) were mixed in glass vessels in air. Up to eight vessels were placed in an Endeavor parallel screening apparatus and flushed with nitrogen. CH_2Cl_2 was added (5 cm^3), and the apparatus was sealed. The vessels were then purged 10 times with nitrogen and once with hydrogen. The autoclave was pressurized with hydrogen (1, 5, or 25 bar), and gas uptake was monitored. After hydrogen uptake was complete (usually within 1 h), the reaction solutions were filtered through a small plug of silica to remove the catalyst. Volatiles were removed on a rotary evaporator, and the conversion was measured by ^1H NMR spectroscopy. The products were characterized by GC for substrate **B** and HPLC for **C**−**F** using the following conditions. For substrate **B**, Varian Chiracel-L-Val column (25 m × 0.25 mm × 0.12 μm), He (carrier) 1.5 cm^3/min, 160 °C; for substrate **C**, Chiracel OJ column (250 mm × 4.6 mm), hexane/^{i}PrOH, 80:20; for substrates **D** and **E**, Chiralpak-AD (250 mm × 4.6 mm), hexane/^{i}PrOH, 70:10; for substrate **F**: HPLC, Chiralpak-AD (250 mm × 4.6 mm); hexane/^{i}PrOH, 90:10.

X-ray Experimental. X-Ray diffraction experiments on crystals of **1a** as its MeCN solvate were carried out at 193(2) K on a Bruker SMART diffractometer using Mo Kα X-radiation (λ = 0.71073 Å) and a single crystal coated in paraffin oil mounted on a glass fiber.[41] Diffracted intensities were integrated[42] from several series of exposures, each exposure covering 0.3° in ω. Absorption corrections were based on multiple and symmetry-equivalent measurements SADABS,[43] and structures were refined using SHELXTL[44] against all F_o^2 data with hydrogen atoms riding in calculated positions, with isotropic displacement parameters equal to 1.2 times the U_{iso} for their attached carbon. Complex neutral-atom scattering factors were used.[45] The crystal structure contained residual electron density which could not be fully identified and was modeled using the SQUEEZE algorithm incorporated into the PLATON suite.

Acknowledgment. We thank Prof. J. G. de Vries, Dr. A. H. M. de Vries, and Dr. J. A. F. Boogers of DSM Chemicals for useful discussions, assistance with the catalytic experiments and ee determinations. D.W.N. thanks the Natural Sciences and Engineering Research Council of Canada (NSERC) and The Royal Society for Postdoctoral Fellowships.

Supporting Information Available: Crystallographic information in CIF format. This material is available free of charge via the Internet at http://pubs.acs.org.

JA800858X

(41) SMART diffractometer control software. *SMART collections: version 5.054*; Bruker-AXS Inc.: Madison, WI, 1997–1998; *SMART APEX collections: version 5.628*; Bruker-AXS Inc.: Madison, WI, 2005; *PROTEUM collections: version 5.625*; Bruker-AXS Inc.: Madison, WI, 1997–2001.
(42) *SAINT V6.02–7.06A integration software*; Siemens Analytical X-ray Instruments Inc.: Madison, WI, 2003.
(43) Sheldrick, G. M. *SADABS V2.10*; University of Göttingen: Göttingen, Germany, 2003.
(44) *SHELXTL program system*, version 5.1; Bruker Analytical X-ray Instruments Inc.: Madison, WI, 1998.
(45) *International Tables for Crystallography*: Kluwer: Dordrecht, 1992; Vol. C.